

# Multimodality Texture Analysis

## 1. Introduction

Quantitative imaging biomarkers are increasingly used in cancer imaging to identify tumor stage and aggressiveness. One of the most promising biomarkers is image texture – a quantitative measure of spatially organized, quasi-periodic patterns, or granulations, with a specific brightness and smoothness. The texture feature vector derived from the signal within the tumor in combination with clinical and genetic information may be useful in predicting disease aggressiveness and outcome.

This team at NYU Radiology has established a strong association between texture measured using MRI, PET, and CT images and histological characteristics of the kidney, prostate, and breast tumors [1-11]. These and other studies provide increasing evidence that image texture reflects the underlying properties of cancer that may be used to support clinical decisions and improve patient care. FireVoxel contains analytical tools for computing texture feature vector for individual images and batch processing.

## 2. Texture Analysis in FireVoxel

FireVoxel's texture analysis algorithm mimics the biological patterns of cancer growth by separating the tumor and the surrounding region into concentric 3D shells (Fig. 1). This approach enables capturing the spatial variation of texture features that cannot be obtained by conventional methods. The software combines texture from all available images, such as images acquired by multiple modalities as well as computed parametric maps.

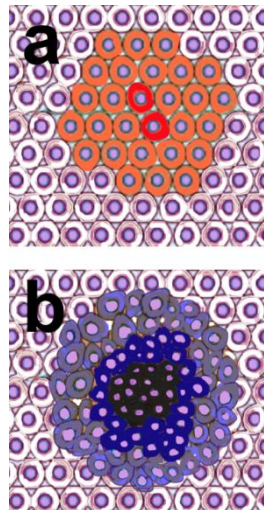


*Figure 1. Schematic of cancer growth.*  
**a.** The growth of the tumor (orange) within the normal tissue (white/purple) is initiated when one or more mutated cells (red) begin to proliferate abnormally. Further mutations result in increasingly rapid progression of cancer.  
**b.** Advanced tumor exhibits proliferating cells in the outer layer (gray), a quiescent inner ring (blue) and a necrotic core (black). Necrosis results from a limited supply of oxygen and nutrients and accumulation of waste products. These concentric patterns are often reflected in 3D tomographic images.

## 3. Algorithm

To generate the texture feature vector, FireVoxel's algorithm executes nested loops L1-L4:

```
L1: for each imaging modality
  L2: for each volume of interest (VOI)
    L3: for each spatial scale or "filter size"
      L4: for each concentric inner & outer ring
        compute signal characteristics & append to feature vector
```

Here promising modalities may include CT and MRI, as well as MRI-derived maps of the apparent diffusion coefficient (ADC) and volume transfer constant  $K^{trans}$ . The L4 loop may include the surrounding rings, the inner ring, and the remaining core (Fig. 2). The L3 loop includes the original image and various

filtered versions at a given feature size (Fig. 3).

The computed signal characteristics include the mean, standard deviation, skewness, kurtosis, and entropy.

FireVoxel's texture analysis tool introduces optional 3D image filters that modify the original image. The dual goal of filtering is to (a) extract features of given granularity size (Fig. 3); and (b) suppress image artifacts. The current texture-sensitive filtering is based on the analysis of a spherical vicinity  $S$  of each voxel. FireVoxel's algorithm considers all possible splits of  $S$  into two hemispheres  $\{S+, S-\}$  and identifies one in which these hemispheres have the most distinct histograms. Histograms are compared using either a simple bin-by-bin difference or a sophisticated Earth Mover Distance method [12]. This yields at each voxel the texture gradient with the magnitude equal to the largest difference between histograms.

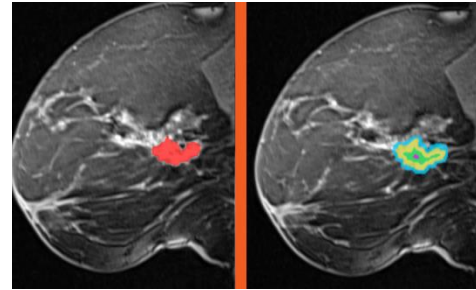


Figure 2. Fat-suppressed T1-weighted 3D breast MRI. The lesion is segmented as a whole (left) and then split into concentric rings (right) for texture analysis. Segmentation regions:

*red:* whole lesion  
*blue:* outer ring  
*yellow:* inner ring 1  
*green:* inner ring 2  
*brown:* core

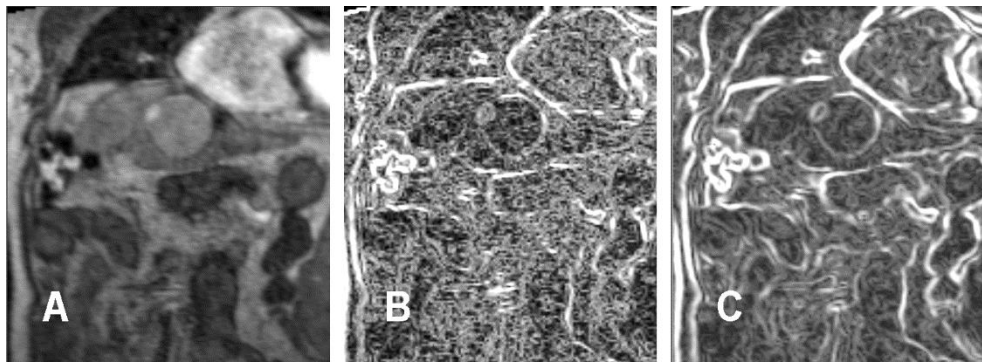


Figure 3. Feature identification on MRI image by 3D filtering. A: original image; B: the same image filtered by texture gradient sensitized to 1-mm features; C: image filtered and sensitized to 3-mm features.

## 4. Batch Tool

FireVoxel's batch tool enables performing texture analysis on a collection of cases in one source folder. All study cases must be saved as FireVoxel documents (\*.fvx), which allows saving multiple coregistered images and ROI masks in a single file. It is important to name imaging modalities and ROIs consistently across the study for easier identification of the results.

With no images loaded, select **Applications > Region Heterogeneity Analysis Batch process** (Fig. 4). This opens the dialog to configure the analysis (Fig. 5). The settings in this dialog are described below.

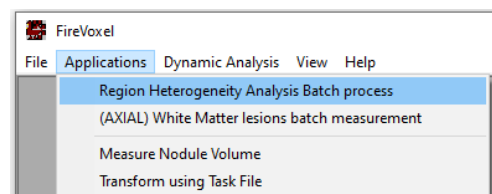


Figure 4. FireVoxel's batch tool for texture analysis is available when no images are loaded.

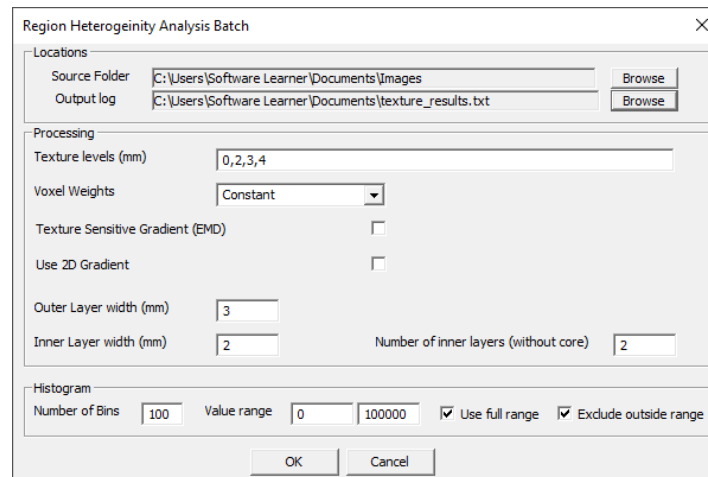


Figure 5. Region Heterogeneity Analysis Batch dialog.

**Source Folder** – To specify the source directory, click Browse to open browse-for-folder dialog and select the directory of the study cases. The source directory must contain all study cases saved as FireVoxel documents (.fvx).

**Output log** – To specify the output file, click Browse to open save-as dialog, navigate to the target location and enter a file name (\*.txt). The output file will show the path to the source directory and the processing settings from this dialog. The results are presented as a tab-delimited table, with each layer from each case in a separate row and the following columns: case ID, modality, ROI (shell), texture radius, ROI volume, and ROI parameters (mean, standard deviation, skewness, kurtosis, and entropy).

**Texture levels (mm)** – Parameters describing automatically created texture filters that will be applied to all image layers. For example, if interested in analyzing 1) the original image and 2) a 3-mm filtered image that enhances 3-mm-size features, enter 0,3 in this box. Note that filtering can be time-consuming, so for the initial testing, skip filtering and enter 0.

**Voxel Weights** (drop-down menu), **Texture Sensitive Gradient (EMD)** (checkbox), **2D** (checkbox) – Filter parameters. The options for Voxel Weights include Constant (default), Gaussian, Radial, and Rayleigh. Users may wish to start with the default settings (Constant, No, No).

**Outer layer width (mm)** – If not zero, the program will automatically create a 3D region of the specified thickness. This ROI is located just outside the lesion. The histogram features for this region will be labeled: `lesion_or`, where `lesion` is the name of the main (whole-lesion) ROI.

**Number of inner layers** – If not zero, the program will automatically create the specified number of inner layers, or rings. These concentric rings are all located inside the lesion. The histogram features for the first ring will be labeled `lesion_ir1`; for the second ring, `lesion_ir2`, etc. The algorithm will also segment the inner core – the area remaining after all of rings are subtracted from the whole-lesion ROI. The histogram features for the core are labeled `lesion_co`.

**Inner layer width (mm)** – The thickness (in mm) of each ring. When selecting the ring thickness and the number of rings, consider the smallest lesion size in the study. Some rings may end up being empty if the layer thickness is too large.

**Histogram** – Histogram parameters for the analysis. Note that these settings will impact the computed results. Prior to the analysis, these parameters may need to be tested and selected interactively in **Layer Control > ROI Stats 3D** (Fig. 6).

- **Number of Bins** – The number of bins in histogram (default, 100, as in ROI Stats 3D).
- **Value range** (min and max values) – The minimum and maximum values of the range of the histogram. The default is [0, 100000]. In ROI Stats 3D dialog, the default range is set to the full range of data within the ROI, between the lowest and the highest values.
- **Use full range** (checkbox) – Has the same effect as the Full button in ROI Stats 3D. Expands the range to include the full range of data between the lowest and highest data values.
- **Exclude outside** (checkbox) – Has the same effect as Clip checkbox in ROI Stats 3D. If checked, the data outside the value range are excluded.

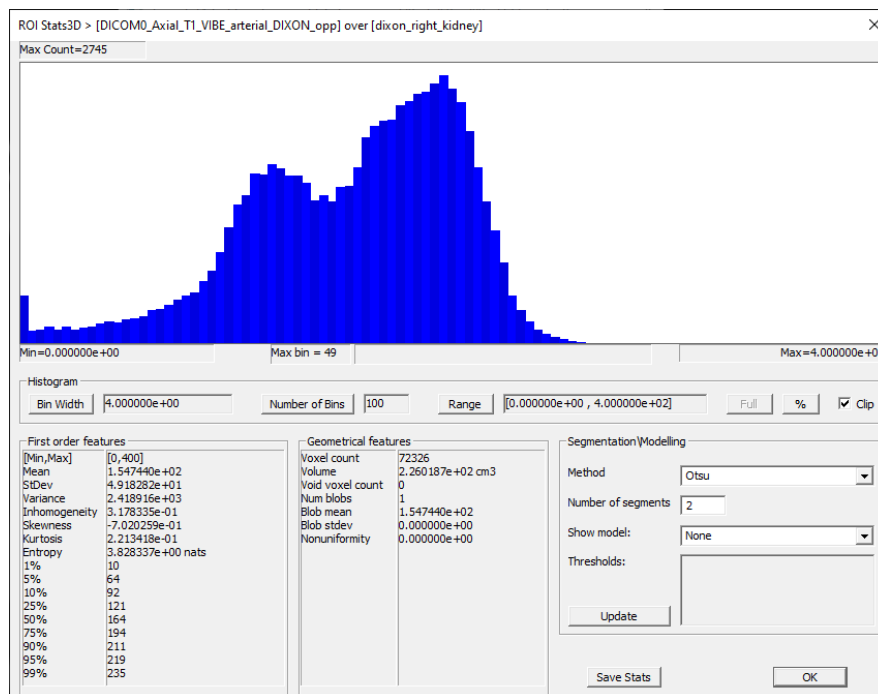


Figure 6. ROI Stats 3D dialog showing the histogram of signal within an ROI and the histogram parameters: **Number of Bins**, **Range**, **Full** (range), and **Clip**. The resulting histogram features are listed under **First order features** and the **Geometrical features**.

---

## References

1. Dittmer-Roche B, Rusinek H, Ko JP, McGuinness G, Naidich D. Automated assessment of small airway disease on lung CT. *SPIE Medical Imaging: Image Processing*, Vol. 5030, 403-13, 2003.
2. Doshi AM, Ream JM, Kierans AS, Bilbily M, Rusinek H, Huang W, Chandarana H. Use of MRI in differentiation of papillary renal cell carcinoma subtypes: Qualitative and quantitative analysis. *AJR Am J Roentgenol* 206(3):566-72, 2016. PMID: 26901013.
3. Kierans AS, Bennett GL, Mussi TC, Babb JS, Rusinek H, Melamed J, Rosenkrantz AB. Characterization of malignancy of adnexal lesions using ADC entropy: comparison with mean ADC and qualitative DWI assessment. *J Magn Reson Imaging* 37(1):164-71, 2013. PMID: 23188749.
4. Kierans AS, Rusinek H, Lee A, Shaikh MB, Triolo M, Huang WC, Chandarana H. Textural differences in apparent diffusion coefficient between low- and high-stage clear cell renal cell carcinoma. *AJR Am J Roentgenol* 203(6):W637-44, 2014. PMID: 25415729.
5. Ko JP, Suh J, Ibdapo O, Escalon JG, Li J, Pass H, Naidich DP, Crawford B, Tsai EB, Koo CW, Mikheev A, Rusinek H. Lung adenocarcinoma: Correlation of quantitative CT findings with pathologic findings. *Radiology* 280(3):931-9, 2016. PMID: 27097236.
6. Pires A, Rusinek H, Suh J, Naidich DP, Pass H, Ko JP. Clustering of lung adenocarcinomas classes using automated texture analysis on CT images. *Proc SPIE Vol. 8669, 25-32, Medical Imaging 2013: Computer-Aided Diagnosis*. Nico Karssemeijer, Ronald M. Summers, Eds.
7. Rosenkrantz AB, Obele C, Rusinek H, Balar AV, Huang WC, Deng FM, Ream JM. Whole-lesion diffusion metrics for assessment of bladder cancer aggressiveness. *Abdom Imaging* 40(2):327-32, 2015. PMID: 25106502.
8. Rosenkrantz AB, Triolo MJ, Melamed J, Rusinek H, Taneja SS, Deng FM. Whole-lesion apparent diffusion coefficient metrics as a marker of percentage Gleason 4 component within Gleason 7 prostate cancer at radical prostatectomy. *J Magn Reson Imaging* 41(3):708-14, 2015.
9. Rosenkrantz AB, Ream JM, Nolan P, Rusinek H, Deng FM, Taneja SS. Prostate cancer: Utility of whole-lesion apparent diffusion coefficient metrics for prediction of biochemical recurrence following radical prostatectomy. *AJR Am J Roentgenol* 205(6):1208-14, 2015. PMID: 24616064.
10. Rosenkrantz AB, Meng X, Ream JM, Babb JS, Deng FM, Rusinek H, Huang WC, Lepor H, Taneja SS. Likert score 3 prostate lesions: Association between whole-lesion ADC metrics and pathologic findings at MRI/ultrasound fusion targeted biopsy. *J Magn Reson Imaging* 43(2):325-32, 2016. PMID: 26131965.
11. Stember JN, Ko JP, Naidich DP, Kaur M, Rusinek H. The self-overlap method for assessment of lung nodule morphology in chest CT. *J Digit Imaging* 26(2):239-47, 2013. PMID: 23065123.
12. Rubner Y, Tomasi C, Guibas LJ. The earth mover's distance as a metric for image retrieval. *Int J Comput Vis* 40(2): 99-121, 2000.

